Field emitters based on porous aluminum oxide templates

D. N. Davydov,[a] P. A. Sattari, D. AlMawlawi, A. Osika, T. L. Haslett, and M. Moskovits
Department of Chemistry, University of Toronto, and Photonics Research Ontario, 80 St. George St., Toronto, Ontario, Canada M5S 3H6

(Received 26 October 1998; accepted for publication 24 June 1999)

The field-emission properties of cold cathodes produced using nano-porous anodic aluminum oxide (AAO) templates are reported. Several types of field emitters were fabricated: aligned copper nanowires grown halfway up the parallel nano-pores of the AAO; aligned multiwalled carbon nanotubes grown to the top of the pores; surfaces overgrown with random tangles of carbon nanotubes; and empty AAO templates. Significant field-emission currents (field enhancement values ~ 1800) were obtained at threshold voltages as low as 80 V (corresponding to fields of 3–4 V/μm) on samples of nanotube tangles. Perfectly aligned carbon nanotubes were less efficient field emitters and had lower field enhancement values. These observations are explained in terms of the mean separation of active tips in the two sets of samples. Empty templates and metal nanowire arrays show lower field enhancements and higher threshold electric fields (40–70 V/μm). In these samples significant field-emission currents are produced at relatively low applied voltages of 110–300 V due to the small inter-electrode separations achieved on depositing a metal grid directly on the surface of the porous template. © *1999 American Institute of Physics.* [S0021-8979(99)04519-3]

I. INTRODUCTION

Field-emission devices with low threshold voltages are potentially useful as electron emitters in flat panel displays. The current emphasis in that field has been on using diamond-coated nano-tips[1] and silicon microtip cathodes.[2,3] Recently, field emitters based on carbon nanotubes[4–6] have been the subject of considerable study. An alternative approach that could potentially be used to create low-voltage field emitter arrays is based on reported methods for fabricating arrays of parallel metal nanotips[7–9] and multiwalled carbon nanotubes[10] within anodic aluminum oxide (AAO) nano-templates. AAO self-organizes into a hexagonal array of uniform nano-pores[11] with pore densities of up to $10^{12}\,\mathrm{cm}^{-2}$ and pore diameters ranging from approximately 4 to >300 nm. A variety of nano-tip structures can be fabricated using AAO templates by depositing metals or synthesizing carbon nanotubes in the pores followed by procedures to make electrical contacts to the arrays.

Carbon nanotubes possess interesting structural and electronic properties that suggest a number of useful applications. The small radii of curvature of their tips and their high stability make them obvious candidates as field-emission electron sources.[4–6,12] Several field-emission studies reported for single- and multiwalled carbon nanotube films[12] and nanotube bundles[5,6] demonstrate the capability of carbon nanotubes to emit electrons with a high current density and threshold electric fields in the range 1–10 V/μm.

Recently, a technique was reported for producing multiwalled carbon nanotube arrays by pyrolyzing a hydrocarbon in the nano-pores of an anodic aluminum oxide template.[10] Using this method, aligned arrays of carbon nanotubes can be fabricated with densities of up to $10^{12}\,\mathrm{cm}^{-2}$ and highly uniform diameters [diameter distributions with full width at half maximum (FWHM) ~12% of the mean diameter].

In this article we report the successful development of field-emission electron sources using AAO templates. The field-emission characteristics of multiwalled carbon nanotubes pyrolytically grown in porous AAO templates and overlaid with standard copper mesh grids are presented in Sec. II. The field-emission electric field and field enhancement for the nanotube samples are shown to be strongly affected by the nanotubes' structure which, in turn, is shown to depend on the growth conditions and surface treatment.

Field emitters based on empty AAO templates and templates partially filled with metal nanowires are described in the Sec. III. The high electric fields needed to emit electrons from the nanowire arrays are produced between the tips of the metal nanowires and a thin metal grid vapor deposited obliquely directly on top of the AAO template such that the mouths of the pores are not completely blocked. Because the thickness of the AAO templates is of the order of a few micrometers, strong electric fields are created at low applied voltages.

II. CARBON NANOTUBE ARRAYS

The AAO templates were prepared as described previously.[7] Pure Al sheets, approximately 0.2 mm thick, were electrochemically polished in aqueous perchloric acid/ethanol/2-butoxy ethanol solutions and anodized for approximately 25 min in 0.3 M oxalic acid at 19 °C with 50 V dc using a graphite counter electrode. The resulting porous aluminum oxide possesses uniform, parallel pores approximately 40 nm in diameter and 5–6 μm long. Cobalt nanoparticles approximately 100 nm in length were electrochemically deposited at the bottom of the pores at 15 V ac

[a]Electronic mail: ddavydov@chem.utoranto.ca

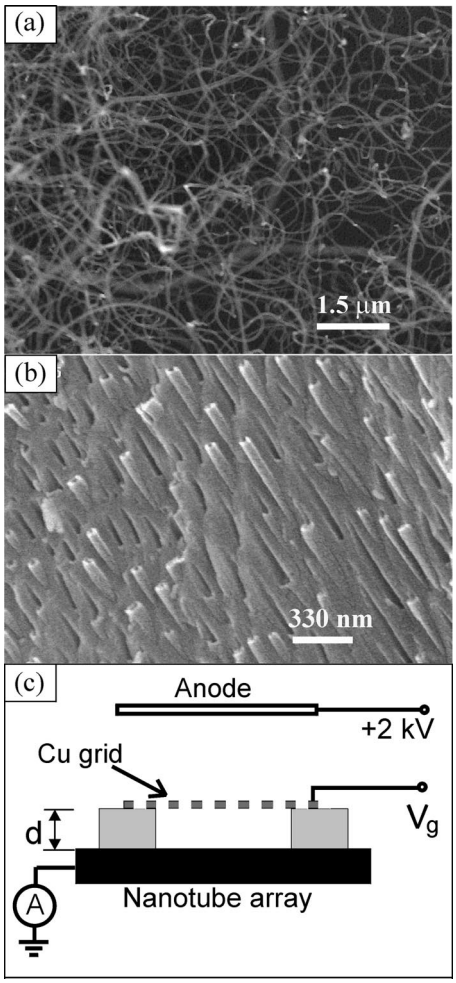

FIG. 1. (a) SEM images of the field-emission sample surface with a random overgrowth of nanotubes; (b) SEM image of a field-emission sample with aligned carbon nanotubes; (c) schematic of a field emission measurement setup.

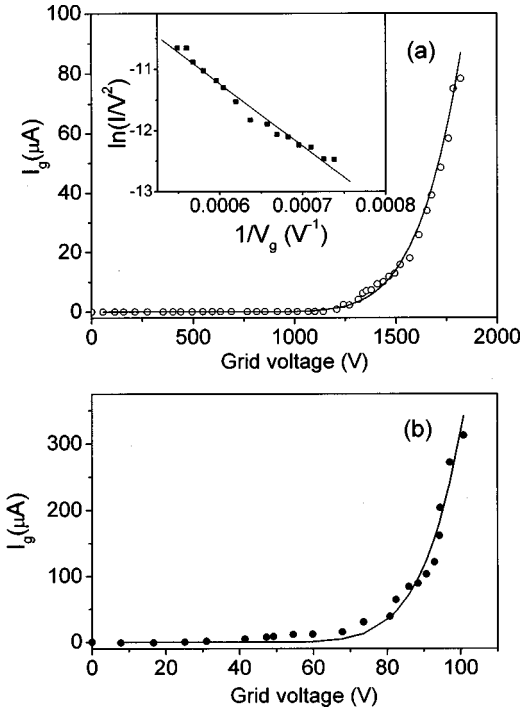

FIG. 2. *I–V* field-emission curves obtained from a sample whose surface was covered with random carbon nanotube tangles for grid-surface separations of (a) 360 μm and (b) 25 μm. Points are experimental measurements; solid lines are the fits to the Fowler–Nordheim formula.

using a Co sulfate electrolyte stabilized with boric and ascorbic acids.[10] Multiwalled carbon nanotubes were then grown inside the pores by catalytically pyrolyzing acetylene for ~20 min at 700 °C using a 10% acetylene in nitrogen feed gas at rates of 100 ml/min in a flow reactor. Following synthesis, the nanotubes were annealed for 15 h at 700 °C in a pure N_2 flow in order to promote graphitization. The nanotubes grew from the (closed) bottom of the pores to the (open) top. Field-emission characteristics were determined for samples prepared with varying pyrolysis times.

Electron microscopy revealed that for the shortest pyrolysis times used the nanotubes did not reach the template surface. At the highest pyrolysis times, the nanotubes grow out of the pores, creating a random tangle of nanotubes on the surface [Fig. 1(a)]. The nanotube diameters were approximately equal to the pore diameter even when the nanotube growth was no longer confined within the pores. Conditions were also found that yielded tubes that stopped growing when they reached the top of the pore. Briefly etching the AAO with NaOH slightly exposes the tips of the nanotubes from their AAO template [Fig. 1(b)].

Standard high transmission copper grids (hexagonal, 600 mesh) were glued with epoxy at heights in the range 25–360 μm above the sample surface using various insulating spacers. A positive voltage was applied to the grid and the field-emission current was measured at a phosphorescent cathode. The experiment is shown schematically in Fig. 1(c).

The field-emission data were analyzed using the Fowler–Nordheim formula $I \sim E^2 \exp(A\phi^{3/2}/E)$, where ϕ (~ 4 eV) is the work function, the constant $A = 6.83 \times 10^{-9}$, and the electric field is given by $E = \beta V/d$, where d is the anode to cathode distance and β is the so-called field enhancement factor. Two field-emission *I–V* curves are shown in Fig. 2 for a sample ''overgrown'' with nanotubes [see Fig. 1 (a)]. The two curves correspond to different portions of the same sample with grid-sample surface separations of 360 ± 10 and 25 ± 7 μm. Despite the chaotic nanotip arrangement, both curves are stable and reproducible with relatively low threshold electric field values of ~ 3–4 V/μm. The field enhancement values obtained from the Fowler–Nordheim plots were similar as expected, at $\beta \sim 1900$ [Fig. 2(a)] and $\beta \sim 1600$ [Fig. 2(b)]. The scanning electron microscopy SEM micrographs [Fig. 1(a)] indicate that there are sharp kinks within the chaotic tangle of nanotubes on the surface. It is likely that these are the reason for the field enhancement values observed.

In the second set of samples, the nanotube lengths corresponded approximately to the AAO template thickness [Fig. 1(b)]. For these samples, a grid-surface separation of 25 ± 7 μm yielded the current–voltage (*I–V*) curve shown in Fig. 3. Higher electric field thresholds in the range 30–45 V/μm were required for field emission with these samples, (i.e.), an order of magnitude greater than with the randomly oriented (chaotic) nanotubes. The field enhancement factor

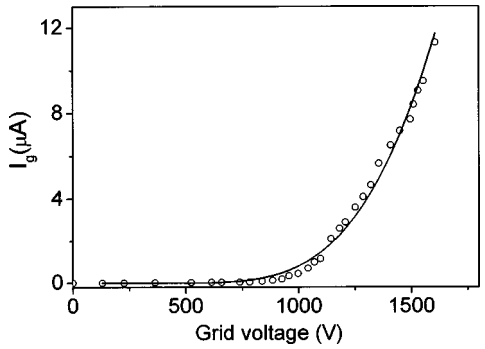

FIG. 3. *I–V* field-emission characteristics for samples prepared with aligned nanotube arrays. Points are measured data; solid line is the best fit to the Fowler–Nordheim formula.

of $\beta \sim 300$ for the aligned nanotube array was also considerably smaller than for the chaotic nanotubes.

The robustness of the measurements was confirmed by repeating them at several spots on the rather large samples produced. The current values were reproducible within ~15% over the set of samples. At very high voltages (higher than those shown in Figs. 2 and 3), the field-emission currents sometimes became unstable, at times fluctuating by more than an order of magnitude.

The striking differences in the threshold electric field values and the field enhancement factors obtained with the two types of nanotube samples are likely due to the density of active field-emission tips. For the aligned nanotubes, the field enhancement is low owing to the high density of tips ($\sim 4\times 10^{12}\,\mathrm{cm}^{-2}$) leading to efficient field screening—the average inter-tube separation is of the order of 150 nm, while the distance between the grid and the sample surface is tens of micrometers. For the overgrown, chaotic nanotubes, the number of active tips, i.e., those with the greatest curvature, are rather small. It is likely that only those nanotubes in which the tube growth ''doubles up'' on itself and those with broken ends contribute significantly to the field emission. These sharp tips are visible in Fig. 1(a).

III. POROUS AAO TEMPLATES

In this section we describe field emitters based on empty AAO templates and templates partially filled with metal nanowires. In contrast to the standard copper grids used in the field-emission studies on the carbon nanotube samples, the grids used with the metal nanowire samples were Ag films directly deposited on the AAO template surface. This strategy, made possible because the conducting portion of the sample does not reach the AAO surface and cause electrical shorts, results in an inter-electrode separation, *d*, of the order of only a few μm, thereby ensuring high electric fields regardless of the field enhancement. Beyond the grid, the field-emitted electrons were collected on a phosphor screen anode held at an accelerating voltage of 1.6 kV.

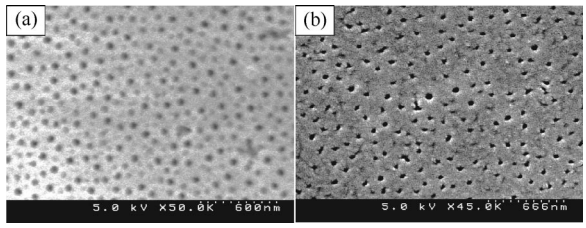

FIG. 5. (a) Top-view SEM micrograph of the porous AAO template; (b) SEM micrograph of the Ag grid deposited on the AAO surface.

Typically, nano-templates of thickness 5–6 μm containing 30–40-nm-diameter pores were fabricated by anodizing Al in oxalic acid at 50 V. The porous portion of the AAO film is separated from the underlying, bulk aluminum by a thin aluminum oxide barrier layer whose thickness is approximately proportional to the anodizing voltage used to fabricate the template. At the end of the anodization process, the voltage can be gradually reduced so as to reduce the barrier layer thickness. After anodizing, the pore diameter was increased to a mean diameter in the range 50–80 nm by etching the templates in phosphoric acid at room temperature for 2 h. The pore widening also removed debris from the interior of the pore, thus promoting metal deposition.

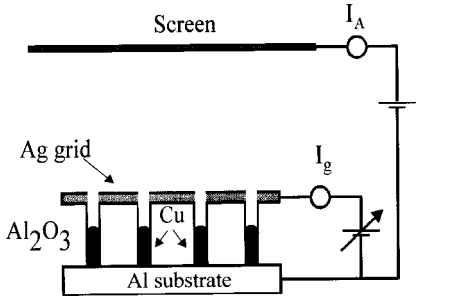

FIG. 4. Schematic view of the metal nanowire-based field emitter.

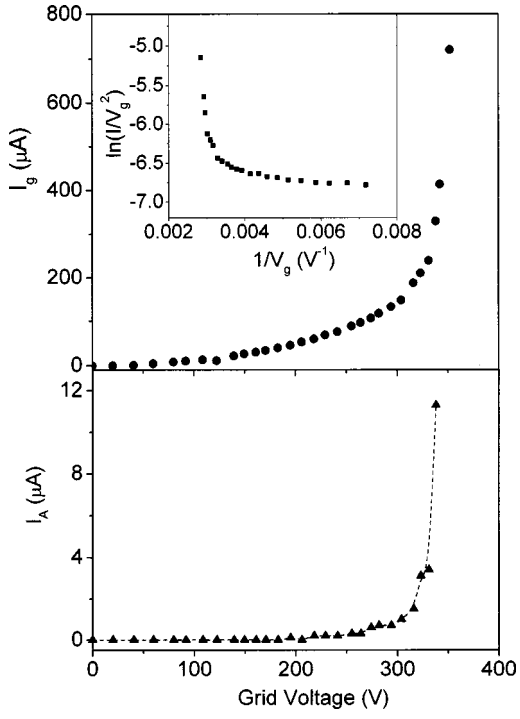

FIG. 6. The grid (a) and the anode (b) current vs grid voltage for a 5-μm-thick AAO template with 80 nm pore diameter. Inset: Fowler–Nordheim $\ln(I_g/V_g^2)$ vs $(1/V_g)$ plot.

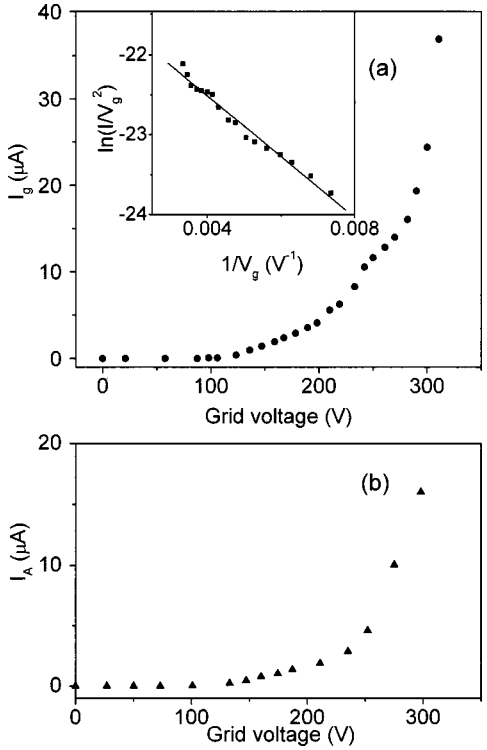

FIG. 7. The grid (a) and the anode (b) current vs the grid voltage for a 6-μm-thick template with empty pores (average pore diameter of 60 nm). Inset: Fowler–Nordheim plot for the grid current.

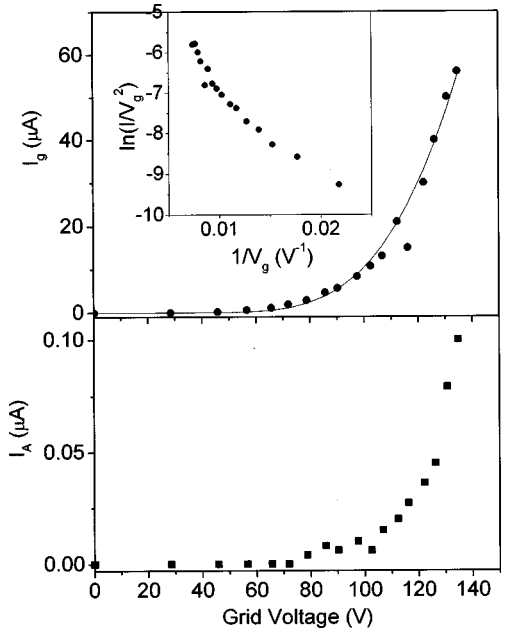

FIG. 8. Grid (a) and anode (b) current vs grid voltage for a 5-μm-thick sample with pores partially filled with Cu nanowires. Points are experimental measurements; solid line is the fit to the Fowler–Nordheim formula. Inset: Fowler–Nordheim plot for the grid current.

The field-emission experiment is shown schematically in Fig. 4. Two types of samples were used in the course of these experiments. In the first, a thin Ag film (150–200 nm) was vapor deposited on the porous surface of an empty AAO template at an angle of 30° with respect to the surface plane, thereby producing an electrically continuous low-resistance film which nevertheless retained most of the pore mouths open [Fig. 5(b)]. In the second type of sample, Cu nanowires were electrochemically deposited into the pores prior to depositing the Ag grid. The average length of the nanowires was approximately 2.5 μm so that they filled the template to more or less half its thickness. Nanowires were fabricated using well-known ac electrolysis techniques.[7–9]

The characteristics of the Ag grid were greatly dependent on pore diameter. Optimal results were obtained with pore diameters in the range of 50–90 nm. With narrower pores the deposition of the Ag grid sealed most of the pore mouths, while with bigger pores the percolation of the silver on the porous surface was difficult to achieve. In fact, with the largest pores (120–150 nm) conductive silver grids could not be prepared even with films of mean thickness ~1 μm.

A few I–V curves obtained with AAO samples with metal-free pores are shown in Figs. 6 and 7. Figure 6 shows the grid (I_g) and anode (I_A) currents of a 5-μm-thick oxide sample with 80 nm average diameter pores. A similar result obtained with empty 60 nm average diameter pores, approximately 6 μm long, is shown in Fig. 7. For both samples, field-emission anode currents in the range of μA were observed with grid voltages, V_g, in the range 250–300 V (corresponding to electric fields ~50 V/μm).

The transmission efficiency, expressed as the ratio I_A/I_g, was typically in the range ~0.001–0.15. However, in a few exceptional cases this ratio reached 0.4 (Fig. 7). For the data shown in Figs. 6 and 7 these ratios are ~0.03 and 0.4, respectively. This broad range was due to the variation in the degree of pore closure occurring as a result of the Ag grid deposition. Conditions for maximizing this ratio have not yet been optimized but the results indicate that conditions can be achieved in which almost a third of the current extracted from the nanowire tips can pass through the grid to the phosphor screen. In addition to the pore diameter dependence, the degree of pore closure strongly depends on the initial surface roughness of aluminum oxide template. We expect that careful mechanical and electrochemical polishing of the Al prior to anodization would improve the ratio I_A/I_g allowing the deposition of thinner Ag films.

Figure 8 shows an example of field-emission I–V curves for a 5-μm-thick template containing 2.5-μm-long Cu nanowires electrochemically deposited in the pores (topped with a porous silver grid as described above). The field-emission current starts to increase dramatically at V_g ~110 V corresponding to an electric field of 44 V/μm. The field enhancement β was on the order of 400 and the ratio I_A/I_g~0.002.

For most of the samples with deposited Ag grids, the Fowler–Nordheim plot produced two linear portions with an abrupt change in slope (Fig. 6). Field enhancement factors obtained from the slope of the high voltage portion of $\ln(I_g/V_g^2)$ vs $1/V_g$ were found to lie in the range β ~80–800. In the Fowler–Nordheim plots the field strength was assumed to be $E=V_g/d$ where d is the distance between the grid and tips of the nanowire tips or, for samples with no nanowires, the thickness of the AAO template. For the data shown in Fig. 6, β was found to be 80. These values are low

compared to what is reported for field-emission cathodes in the literature.[1–3,5,6] In the low voltage range, β was found to lie in the 6000–9000 range. These are not reasonable values and probably indicate the presence of effects other than field emission. This conclusion is corroborated by the anode current, which for most of the samples did not follow the grid current at low grid voltages (Fig. 6) as would be expected for the case of field emission. The low β values obtained at higher values of V_g may result from the screening effect brought about by the high pore density. The distance from the grid to the Al substrate or to the tips of the Cu nanowires, which ranges from ~2.5 to ~6 μm, is still much larger than the inter-wire separation (~100 nm), although it is better than the situation with the nanotube samples. Strong electric field enhancement is not expected to be observed under such circumstances, especially in the absence of nanowires when the emitting electrode is the flat Al substrate.

The two I–V domains might result from the presence of different emission sites. For example, porous oxide films often have defects such as cracks or holes with dimension much larger than the pore diameters. The electric field strength, E, and the field enhancement factor, β, characterizing the field-emission from such defect sites, could differ markedly from those describing field emission from the nanowires and may lead to the observed anomalies in the Fowler–Nordheim plots. Alternatively and additionally, the two-slope behavior might be related to leakage currents in the insulating aluminum oxide matrix due to the incomplete removal of the electrolyte from the pores. This is suggested by the observation that the current, I_A, detected at the anode starts to increase at higher voltages than the grid current. (See, for example, Fig. 6.) Anomalously low β values observed in the high voltage region could be due to other than Fowler–Nordheim emission sources such as local surface discharges that could occur between nanowires and the Ag grid.

IV. CONCLUSIONS

The current versus voltage field-emission characteristics of nanometer-sized cold cathodes fabricated in porous anodic aluminum oxide templates filled either with carbon nanotubes or metal nanowires were investigated. For comparison, measurements were also carried out on porous templates with empty pores.

Field-emission currents ranging from a few tens to several hundred μA were obtained from nanotube arrays with areas ~2 mm^2 and at voltages as low as 80 V. Samples whose surfaces were covered with random tangles of nanotubes yielded much larger field enhancement factors (β ~1600–1900) and lower threshold electric fields (~3 V/μm) than those obtained for samples with aligned carbon nanotubes (β~300 and threshold fields ~40 V/μm). These observations are explained in terms of the density of active tips in the two sets of samples.

Field-emission cathodes based on AAO templates filled with Cu nanowires or with empty pores and topped with porous metal grids deposited directly on the template surface produced similar grid currents at voltages of 100–300 V, while the currents detected by an anode placed beyond the grid were in the range 0.1–10 μA. The field enhancement in these samples (β~80–800) is considerably lower than that of the samples overgrown with carbon nanotubes. For the nanowire samples the value of threshold electric field was in the range 40–70 V/μm. Despite the low field enhancement characterizing the last set of samples they are, nevertheless, capable of field emitting at relatively low applied voltages due to the implementation of very small inter-electrode separations of only a few μm.

ACKNOWLEDGMENTS

The authors gratefully acknowledge the financial support provided by NSERC through the Research and the NRC/NSERC grant programs. They also thank J. Li for his help in the preparation of the carbon nanotube samples.

[1] C. Nützenadel, O. M. Küttel, O. Gröning, and L. Schlapbach, Appl. Phys. Lett. **69**, 2662 (1996).
[2] C. A. Spindt, I. Brodie, L. Humphrey, and E. R. Westerberg, J. Appl. Phys. **47**, 5248 (1976).
[3] M. Takai, M. Yamashita, H. Wille, S. Yura, S. Horibata, and M. Otobake, Appl. Phys. Lett. **66**, 422 (1995).
[4] W. A. de Heer, A. Châtelain, and D. Ugarte, Science **270**, 1179 (1995).
[5] Q. H. Wang, T. D. Corrigan, J. Y. Dai, R. P. H. Chang, and A. R. Krauss, Appl. Phys. Lett. **70**, 3308 (1997).
[6] P. G. Collins and A. Zettl, Phys. Rev. B **55**, 9391 (1997).
[7] D. AlMawlawi, C. Z. Liu, and M. Moskovits, J. Mater. Res. **9**, 1014 (1994).
[8] A. A. Tager, D. Routkevitch, J. Haruyama, D. AlMawlawi, L. Ryan, M. Moskovits, and J. M. Xu, in *Future Trends in Microelectronics*, NATO ASI Series edited by S. Luryi, J. M. Xu, and A. Zaslavsky (Kluwer Academic Publishers, Dordrecht, 1996), p. 171.
[9] D. Routkevitch, A. A. Tager, J. Haruyama, D. AlMawlawi, M. Moskovits, and J. M. Xu, IEEE Trans. Electron Devices **43**, 1646 (1996).
[10] J. Li, T. L. Haslett, and M. Moskovits, Chem. Mater. **10**, 1963 (1998).
[11] J. A. Switzer, C. J. Hung, B. E. Breyfogle, M. G. Shumsky, R. Van Leeuwen, and T. D. Golden, Science **264**, 1573 (1994).
[12] J.-M. Bonard, J.-P. Salvetat, T. Stöckli, W. de Heer, L. Forró, and A. Châtelain, Appl. Phys. Lett. **73**, 918 (1998).